Large solar energetic particle events of cycle 23: A global view

N. Gopalswamy,[1] S. Yashiro,[1,2] A. Lara,[3] M. L. Kaiser,[1] B. J. Thompson,[1]
P. T. Gallagher,[1,4] and R. A. Howard[5]

Received 10 October 2002; revised 26 November 2002; accepted 10 February 2003; published 24 May 2003.

[1] We report on a study of all the large solar energetic particle (SEP) events that occurred during the minimum to maximum interval of solar cycle 23. The main results are: 1. The occurrence rate of the SEP events, long-wavelength type II bursts and the fast and wide frontside western hemispheric CMEs is quite similar, consistent with the scenario that CME-driven shocks accelerate both protons and electrons; major flares have a much higher rate. 2. The SEP intensity is better correlated with the CME speed than with the X-ray flare class. 3. CMEs associated with high-intensity SEPs are about 4 times more likely to be preceded by wide CMEs from the same solar source region, suggesting the importance of the preconditioning of the eruption region. We use a specific event to demonstrate that preceding eruption from a nearby source can significantly affect the properties of SEPs and type II radio bursts. *INDEX TERMS:* 2118 Interplanetary Physics: Energetic particles, solar; 7513 Solar Physics, Astrophysics, and Astronomy: Coronal mass ejections; 7534 Radio emissions; 7514 Energetic particles. **Citation:** Gopalswamy, N., S. Yashiro, A. Lara, M. L. Kaiser, B. J. Thompson, P. T. Gallagher, and R. A. Howard, Large solar energetic particle events of cycle 23: A global view, *Geophys. Res. Lett.*, *30*(12), 8015, doi:10.1029/2002GL016435, 2003.

1. Introduction

[2] The leading paradigm for gradual solar energetic particles (SEPs) is that they are accelerated by fast mode MHD shocks driven by coronal mass ejections (CMEs) in the outer corona and in the interplanetary (IP) medium [see, e.g., *Reames*, 1999]. Consistent with this paradigm, SEP intensities and CME speeds are correlated, although it is not uncommon to find SEP intensities over a range of 4 orders of magnitude for a given CME speed. At least part of this scatter may be explained by the observation that higher SEP intensities result when the ambient medium has elevated levels of SEPs [*Kahler*, 2001; see also *Van Hollebeke et al.*, 1990]. The occurrence of preceding CMEs along the paths of CME-driven shocks may have much wider implications than just providing seed particles [*Gopalswamy et al.*, 2001, 2002a, 2002b]. In this paper we assess the implications of large-scale CMEs preceding the primary CME on the resulting intensity of SEP events. We also investigate the relation between radio bursts produced by CME-driven shocks, fast and wide CMEs, major solar flares and SEP events as a function of the solar cycle.

2. Data Selection

[3] The starting point of this study is the list of 48 large SEP events with intensity (I) of >10 MeV protons exceeding 10 particle flux units (pfu) that occurred when the Solar and Heliospheric Observatory (SOHO) was observing the CMEs. We collected the measured properties of the associated CMEs and identified the solar longitude of the associated flares using the on-line Solar Geophysical Data as well as data from other inner coronal imagers such as SOHO's Extreme ultraviolet imaging telescope (EIT) and the soft X-ray telescope (SXT) on board Yohkoh. Using the on-line catalog of SOHO CMEs (http://cdaw.gsfc.nasa.gov/CME_list) we gathered the properties of other CMEs that occurred in the vicinity of the primary CMEs. Type II radio bursts associated with the SEP events were detected by the Radio and Plasma Waves (WAVES) experiment [*Bougeret et al.*, 1995] on board Wind spacecraft and are listed in the web site http://www-lep.gsfc.nasa.gov/waves/wavesII.html.

2.1. SEP Occurrence Rate

[4] Figure 1 shows the occurrence rates (per Carrington rotation (CR)) of SEP events, fast and wide frontside western (FWFW) hemispheric CMEs, major solar flares, and the type II bursts in the decameter hectometric (DH) wavelengths. The FWFW CMEs drive shocks, which in turn accelerate electrons and protons. The DH type II bursts are due to electrons accelerated by CME-driven shocks that just depart from the outer corona. The number of FWFW CMEs is comparable to that of the major SEP events during our study period [*Gopalswamy et al.*, 2003]. The occurrence rate of DH type II bursts and FWFW CMEs is roughly the same, and larger than the rate of large SEP events. The DH type II bursts can occur anywhere on the Sun, while the SEP events preferentially occur on the western hemisphere. If we include the minor SEP events, and remove the frontside western hemisphere restriction for the FW CMEs, then all the rates are similar. There was also a general paucity of events for several rotations during 1999 when the tilt of the heliospheric current sheet was maximum. The occurrence rate of major (GOES M and X class) solar flares displays an overall similarity to the DH, SEP and FWFW events as a function of the solar cycle, but differs greatly in details. For example, there were 65 major flares during CR 1982, but there were only 9 DH, 3 SEP and 3 FWFW events.

2.2. CME Speed, Flare Size, and SEP Intensity

[5] One of the basic requirements for shock acceleration is that the CME must be fast enough to drive an MHD

[1]NASA Goddard Space Flight Center, Greenbelt, Maryland, USA.
[2]Also at Institute of Astrophysics and Computational Sciences, Department of Physics, Catholic University of America, Washington, D. C., USA.
[3]Instituto de Geofísica, Universidad Nacional Autónoma de México, México.
[4]Also at L3 Com - Analytics Corporation, Greenbelt, Maryland, USA.
[5]Solar Physics Branch, Space Sciences Division, Naval Research Laboratory, Washington, D. C., USA.

0094-8276/03/2002GL016435

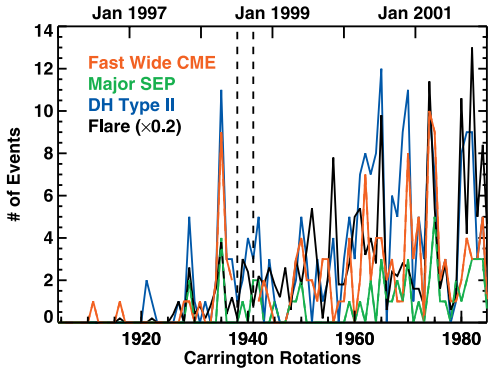

Figure 1. Occurrence rates (per Carrington rotation) of SEPs (red), Fast and Wide Frontside Western (FWFW) CMEs (green), major solar flares (black), and DH type II bursts (blue). No longitude restriction was imposed for flares and DH type II bursts.

shock. Most of the CMEs occur with some level of flare activity especially in soft X-rays. Therefore the three phenomena are closely associated, although the physical relationship is controversial. For the cycle 23 events, the correlation (correlation coefficient r = 0.58, see Figure 2) between the >10 MeV proton intensity and CME speed turns out to be similar to that obtained in previous studies [*Kahler*, 2001]. The lowest intensity is 10 pfu (our selection criterion) and the highest intensity was 31,700 pfu (2001 November 4 event at 17:05 UT). Thus we are dealing with a range of over three orders of magnitude in SEP intensity from CMEs with speeds ranging from 478 km s^{-1} to 2505 km s^{-1}. A significant fraction (15%) of the CMEs had speeds exceeding 2000 km s^{-1}, a population not found in previous studies, probably due to the large field of view of LASCO.

[6] We examined the flare size for the 48 events considered in this study. For 6 events, which occurred from behind the limb, the flare might have been occulted by the limb, so it was not possible to determine the X-ray Class. Of the remaining 42 events, 17 were associated with X-class events while 16 were associated with M-class events. There were 8 C-class events. Some of the C-class events were partly occulted so the assigned class may not reflect the actual size of the flare. Two of the C-class events from the western hemisphere were unambiguous. Thus a large majority (79%) of the major SEP events were associated with large (M or X) flares. There is a weak correlation (r = 0.41) between the X-ray flare size and SEP intensity (see Figure 2). The correlation is somewhat poorer than that between the SEP intensity and CME speed (see Figure 2). This is consistent with the fact that only a small fraction of the major flares is associated with SEP events (see Figure 1).

3. Preconditioning of the Source Region

[7] It was recently found that most of the SEP-associated CMEs are preceded by other CMEs within a few hours suggesting possible interaction within the field of view of the Large Angle and Spectrometric Coronagraph (LASCO) that observes the CMEs [*Gopalswamy et al.*, 2002a]. Large-scale preceding CMEs are likely to produce large changes in the ambient medium above the eruption regions, which we refer to as "preconditioning". In this paper, we consider the effect of wide (width ≥60°) CMEs that departed from the same source region as the primary CME by about a day earlier. Only the fastest CMEs reach 1 AU within a day, so the normal CMEs are likely to have their leading edge somewhere between the Sun and Earth while being connected to the region of eruption on the Sun.

3.1. Preceding CMEs and SEP Intensity

[8] Out of the 48 SEP events, we have excluded 5 events that had uncertain source location or particle flux and used only 43 in the statistics. We divided the 43 events into 18 low (I < 50 pfu) and 25 high (I ≥ 50 pfu) intensity populations. We searched for all the wide (≥60°) preceding CMEs that occurred from the same source region as the primary within the preceding 24 hrs. The times of primary and preceding CMEs, NOAA active region and its location at the time of the primary CME, the time separation (DT) between the primary and preceding CMEs, and the proton flux (pfu) are listed in Table 1. When there were more than one preceding CME within 24 hours, we have listed the one closest to the primary CME. Note that we have not considered narrower (<60°) preceding events. Out of the 19 events in Table 1, 16 are high intensity and are 3 low-intensity events. Thus, 16/25 (64%) of the high-intensity events and 3/18 (17%) of the low-intensity events were preceded by wide CMEs from the same active region as the primary CME. This suggests preconditioning of the ambient medium overlying the source regions of major SEPs may be a factor in deciding the intensity level reached by the SEPs. We have shown the speed and longitude distribution of the highest (>100 pfu) and lowest (<50 pfu) intensity events in Figure 3. The average CME speeds of high- and low-intensity events lie above (1687 km s^{-1}) and below (1261 km s^{-1}) the average (1455 km s^{-1}) speed of all the major SEP events. There is also a significant difference in the longitudes of the high- and low-intensity SEP populations: a larger fraction of the low-intensity events are poorly connected (eastern longitudes and behind the limb cases).

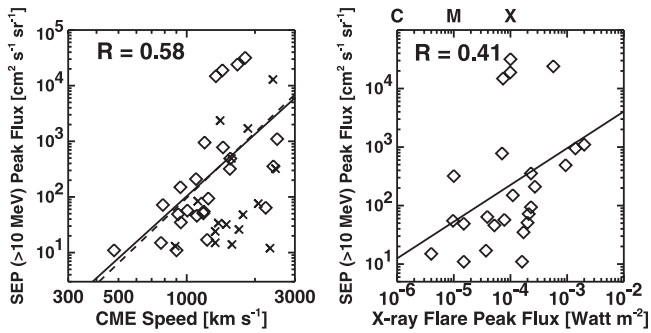

Figure 2. Scatter plot of the SEP intensities of >10 MeV proton events with CME speeds (left) and X-ray flare size (right). All events are plotted in the left panel, but only the 25 events with 0° < longitude < 90° (diamonds) are included in the correlation. The solid lines are best fits to the diamonds. The correlation coefficients are r = 0.58 for CME speeds (confidence level 99.9%) and 0.41 for X-ray flux (confidence level 98%). Excluding the outlier CME with a speed of 478 km s^{-1} results in r = 0.54 (confidence level 99.75%) and the dashed line.

Table 1. SEP Events Preceded by Wide CMEs Within a Day

No.	CME Date/UT	Pre-CME UT	AR	Location	DT[c] (hr)	Flux
1	1997/11/04 06:10	11:11[a]	8100	S14W33	19.0	72
2	1997/11/06 12:10	04:20	8100	S18W63	16.2	490
3	1998/05/02 14:06	05:31	8210	S15W15	8.6	150
4	1998/05/06 08:29	00:02	8210	S11W65	8.4	210
5	1998/05/09 03:35	13:01[a]	8210	S11W90	14.6	12
6	2000/06/06 15:54	15:30	9026	N20E18	0.4	84
7	2000/07/14 10:54	20:30[a]	9077	N22W07	14.4	24000
8	2000/11/08 23:06	22:24[b]	9213	N10W77	<0.3	14800
9	2000/11/24 15:30	05:30	9236	N22W07	10.0	94
10	2000/11/26 17:06	03:30	9236	N18W38	13.6	940
11	2001/03/29 10:26	19:27[a]	9393	N20W19	15.0	35
12	2001/04/02 22:06	12:50	9393	N19W72	9.3	1100
13	2001/04/10 05:30	15:54[a]	9415	S23W09	13.6	355
14	2001/04/12 10:31	13:31[a]	9415	S19W43	21.0	51
15	2001/04/15 14:06	17:54[a]	9415	S20W85	20.2	951
16	2001/04/26 12:30	08:30	9433	N17W31	4.0	57
17	2001/09/24 10:30	21:54[a]	9632	S16E23	12.6	12900
18	2001/10/01 05:30	01:54	9628	S20W90	3.6	2360
19	2001/10/19 16:50	01:27	9661	N15W29	15.4	11

[a]Time corresponds to previous day.
[b]Based on EIT eruption.
[c]Average values = 11.6 hr.

3.2. Interaction of Nearby Eruptions

[9] Figure 4 shows an example of two CMEs that lifted off within three hours of each other. CME1 originated from AR 9704 (S25W67) at 20:30 UT and was associated with the M3.8 flare at 20:18 UT. CME2 appeared above the occulting disk at 23:30 UT and originated from AR 9698 (S15W34, associated with the M9.9 flare at 22:32 UT). The proton

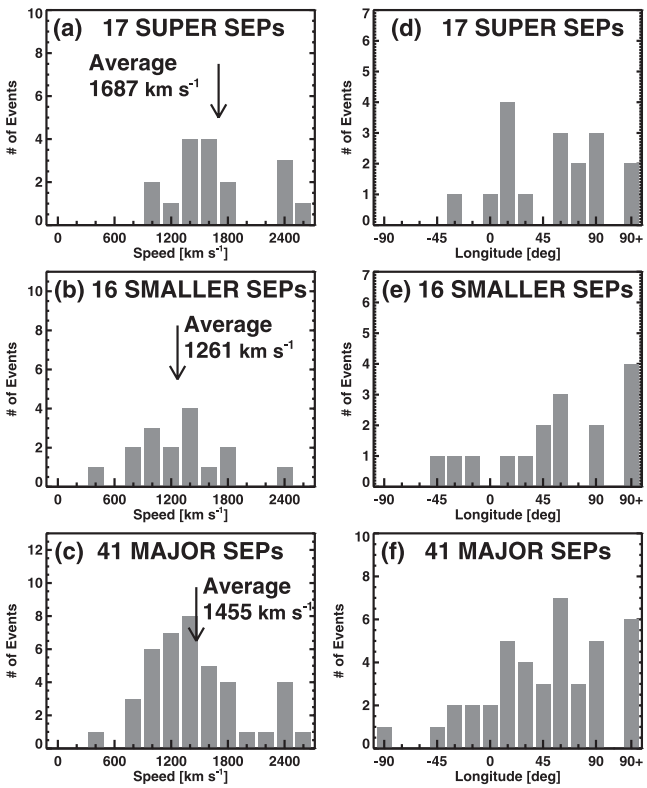

Figure 3. Histograms of speeds (left) and longitudes (right) of high-intensity (SUPER SEPs) and low-intensity (SMALLER SEPs) events compared to all events (MAJOR SEPs).

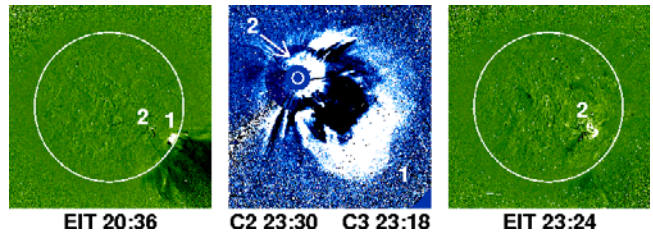

Figure 4. CMEs 1 and 2 observed by SOHO/LASCO as a composite picture using difference images at 23:18 UT (C2) and 23:18 UT (C3) (middle panel) and the source regions from EIT difference images (left and right panels). The white circles represent the optical Sun. CME 2 had occupied the dark region in the middle panel at 22:18 UT.

intensity shows two peaks (marked 1 and 2 in Figure 5) corresponding to the two CMEs. There was also a broad enhancement before the two peaks, probably due to the preceding halo CME from AR 9704 and associated with a gradual flare (marked P in Figure 5). The CME height-time tracks of all the CMEs that preceded the two CMEs illustrate the complexity present in the source region in addition to the interaction between CMEs 1 and 2. Further evidence for CME interaction was found from the Wind/WAVES dynamic spectrum shown in Figure 6. The radio emission associated with the CMEs consists of the two standard features: a set of complex type III bursts and a type II burst. The two CMEs have almost the same speed (1443 km s^{-1} for CME1 and 1437 km s^{-1} for CME2), yet the type II bursts are

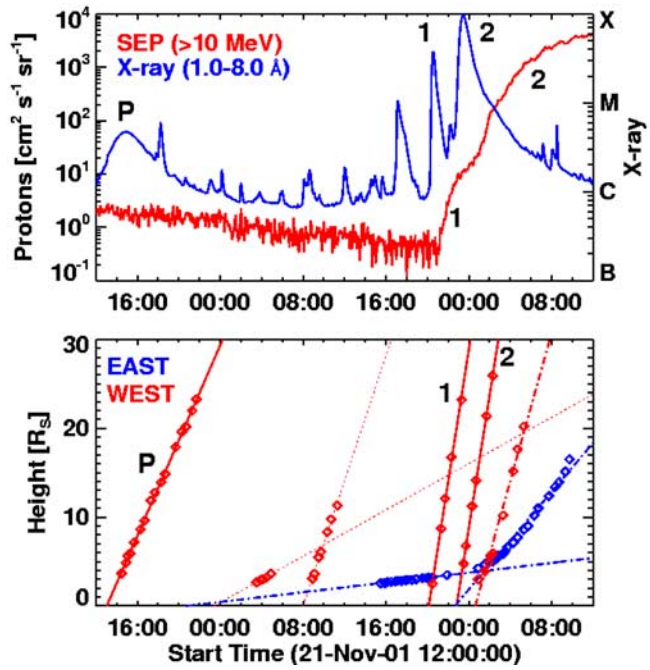

Figure 5. (top) GOES X-ray and proton intensities around the times of the two CMEs (1, 2) on 2001 November 22. The two peaks in the proton intensity and GOES rays corresponding to the CMEs are marked 1 and 2. (bottom) Height-time plots of the all the CMEs that occurred above the east and west limb. CMEs 1, 2 and P are discussed in the text.

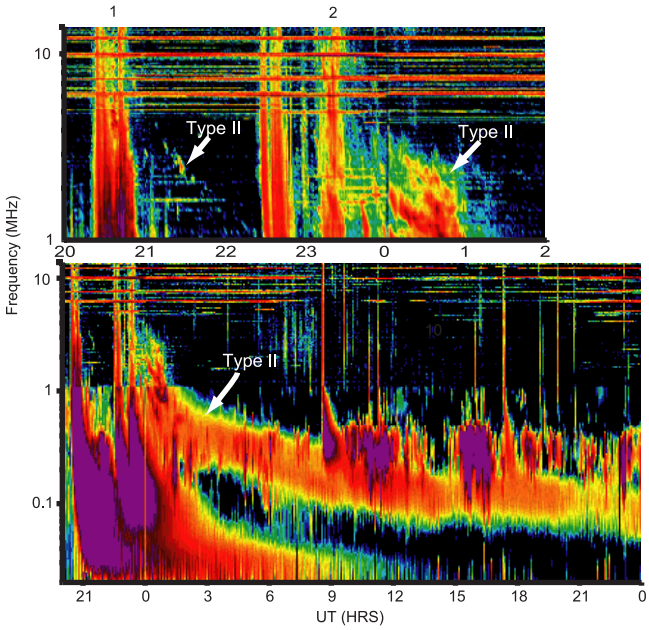

Figure 6. (top) Wind/WAVES dynamic spectrum (1–14 MHz) showing the radio manifestations of the two CMEs (1, 2) of 2001 November 22. An expanded section of the first event is shown on at the top. Type II radio burst (narrow band) from CME1 occurs from 20:30 to 22:30 UT. The second type II starts at 23:00 UT with a huge bandwidth (>100% at 2 MHz) and continues into the low frequency range (bottom panel) beyond the next day. Broad band enhancement is a typical signature of CME interaction.

so different. The first type II is close to a normal one with a band width of ~10% (see *Gopalswamy* [2000] for a type II burst from a noninteracting CME). The second type II is extremely broad band (>100%) with a complex structure. The shock of CME1 is propagating through a normal ambient medium while the shock driven by CME2 is propagating through the material of CME1 - a different ambient medium. Since both CMEs are propagating with roughly the same speed, the relative situation must persist for a long time.

3.3. Influence of Background SEP Intensity

[10] Even though the correlation between pre-event and event SEP intensity is poor (r = 0.15), 37/47 events (79%) had an enhanced background. Of these 37 events, 29 had ambient intensity >0.2 pfu. Thus our analysis supports Kahler's suggestion that enhanced ambient SEP intensity may be one of the factors deciding the intensity of SEPs. We must point out that the intensity of the SEPs from preceding CMEs may be significantly higher near the Sun, which may never be observed at 1 AU, as suggested by *Van Hollebeke et al.* [1990] using Helios 1 measurements at a distance of 0.5 AU from the Sun.

4. Summary and Conclusions

[11] The main results of this study are: 1. The occurrence rates of the SEP events, DH type II bursts and the fast and wide frontside western hemispheric CMEs are quite similar, consistent with the scenario that CME-driven shocks accelerate both protons and electrons. The occurrence rate of major flares, on the other hand, is much higher. DH type II bursts therefore provide an excellent tool for remote sensing SEP-producing CMEs, which constitute only 1–2% of the general population of CMEs. 2. The SEP intensity is slightly better correlated with the CME speed (r = 0.58) than with the X-ray flare size (r = 0.41). The correlation between the SEP intensity and the ambient level of SEPs is rather poor. However, a majority of SEP events (79%) occurred when the ambient level of SEPs was higher than the instrumental threshold. 3. CMEs associated with high-intensity SEPs are about 4 times more likely to be preceded by wide CMEs from the same solar source region. Since the magnetic field lines of the preceding CME are still connected to the Sun, they can return accelerated particles back to the succeeding shock for repeated acceleration, essentially modifying the streaming limit. The preceding CMEs may also stretch the field lines overlying the source region, thus temporarily creating a 'quasi-parallel environment' for the shock of the primary CME. 4. Since CMEs tend to exclude SEPs accelerated by their own shocks, neighboring eruptions are more likely to provide seed particles. CME-driven shocks are extended considerably beyond the confines of the CME itself, which means that eruptions occurring at different locations can influence each other.

[12] **Acknowledgments.** The work was initiated during the Living with a Star (LWS) Coordinated Data Analysis Workshop (CDAW) on Solar Energetic Particles: Solar and Geospace Connections (July 22–26, 2002). The research of SY and AL were supported in part by NSF (ATM 0204588).

References

Bougeret, J.-L., et al., WAVES: The radio and plasma wave investigation on the Wind spacecraft, *Space Sci. Rev.*, *71*, 231–263, 1995.

Gopalswamy, N., Type II solar radio bursts, in *Radio Astronomy at Long Wavelengths*, *Geophys. Monogr.*, vol. 119, edited by R. G. Stone, pp. 123–135, AGU, Washington, D. C., 2000.

Gopalswamy, N., S. Yashiro, M. L. Kaiser, R. A. Howard, and J.-L. Bougeret, Radio signatures of coronal mass ejection interaction: Coronal mass ejection cannibalism?, *Astrophys. J.*, *548*, L91–L94, 2001.

Gopalswamy, N., S. Yashiro, G. Michaek, M. L. Kaiser, R. A. Howard, D. V. Reames, R. Leske, and T. von Rosenvinge, Interacting coronal mass ejections and solar energetic particles, *Astrophys. J.*, *572*, L103–L107, 2002a.

Gopalswamy, N., S. Yashiro, M. L. Kaiser, R. A. Howard, and J.-L. Bougeret, Interplanetary radio emission due to interaction between two coronal mass ejections, *Geophys. Res. Lett.*, *29*(8), 1265, 10.1029/2001GL013606, 2002b.

Gopalswamy, N., S. Yashiro, G. Michalek, M. L. Kaiser, R. A. Howard, R. Leske, T. von Rosenvinge, and D. V. Reames, Effect of CME interactions on the production of solar energetic particles, Solar Wind X, edited by M. Velli, in press, 2003.

Kahler, S. W., The correlation between solar energetic particle peak intensities and speeds of coronal mass ejections: Effects of ambient particle intensities and energy spectra, *J. Geophys. Res.*, *106*, 20,947–20,956, 2001.

Reames, D. V., Particle acceleration at the Sun and in the heliosphere, *Space Sci. Rev.*, *90*, 413–491, 1999.

Van Hollebeke, M. A. I., F. B. McDonald, and J. P. Meyer, Solar energetic particle observations of the 1982 June 3 and 1980 June 21 gamma ray/neutron events, *Astrophys. J.*, *73*, suppl., 285–296, 1990.

P. T. Gallagher, N. Gopalswamy, M. L. Kaiser, B. J. Thompson, and S. Yashiro, NASA Goddard Space Flight Center, Code 695, Greenbelt, MD 20771, USA. (gopals@fugee.gsfc.nasa.gov)

A. Lara, Instituto de Geofisica, UNAM, México D.F. 04510, México.

R. A. Howard, Solar Physics Branch, Space Sciences Division, Naval Research Laboratory, Washington, D. C., 20375, USA.